

Targeting EIF4A1 is effective against human intrahepatic cholangiocarcinoma

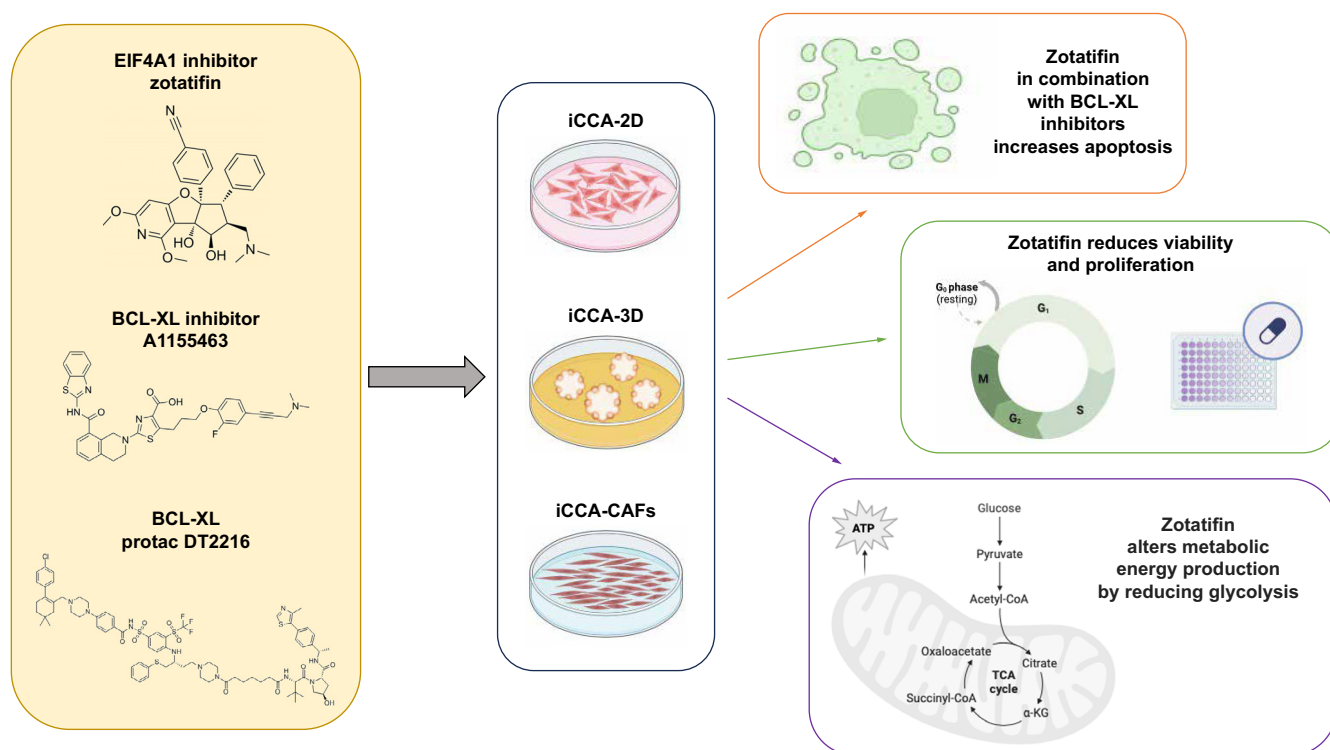
Authors

Wunan Mi, Antonio Cigliano, Grazia Galleri, ..., Luc Johannes Wilhelmus van der Laan, Monique Maria Andrea Verstegen, Diego Francesco Calvisi

Correspondence

calvisid@uniss.it (D.F. Calvisi).

Graphical abstract



Highlights:

- iCCA is an aggressive primary liver tumor with limited therapeutic options.
- EIF4A1 is frequently upregulated in iCCA lesions and correlates with poor patient prognosis.
- Zotatifin, a specific EIF4A1 inhibitor, affects the proliferation of iCCA cells, organoids, and CAFs.
- Zotatifin lowers glycolysis without affecting mitochondrial respiration or inducing morphological mitochondrial alterations.
- Combining zotatifin with inhibitors of the Bcl-xl protein increases apoptosis in iCCA.

Impact and implications:

Dysregulation of the translational machinery is a hallmark of cancer, often linked to tumor progression and poor prognosis. This study underscores the potential of zotatifin, a specific inhibitor of EIF4A1 (an essential component of translation initiation) to inhibit the growth of iCCA cells. In addition, zotatifin demonstrated a synergistic effect when used in combination with the Bcl-xl inhibitors A-1155463 and DT2216, significantly enhancing cell apoptosis. Although this investigation did not include an *in vivo* model, its results, derived from iCCA cell lines, patient-derived organoids, and CAFs, are consistent with the encouraging preliminary results of zotatifin in clinical trials. From a clinical standpoint, these results suggest that zotatifin improves patient outcomes by inhibiting iCCA growth and reducing tumor aggressiveness. Furthermore, combining zotatifin with other drugs could represent a promising therapeutic strategy for targeting iCCA.

<https://doi.org/10.1016/j.jhepr.2025.101416>

© 2025 The Author(s). Published by Elsevier B.V. on behalf of European Association for the Study of the Liver (EASL). This is an open access article under the CC BY-NC-ND license (<http://creativecommons.org/licenses/by-nc-nd/4.0/>). JHEP Reports, 2025, 7, 1–12

Targeting EIF4A1 is effective against human intrahepatic cholangiocarcinoma

Wunan Mi¹, Antonio Cigliano², Grazia Galleri³, Isabella Gigante⁴, Sara Martina Steinmann⁵, Ezgi Cibali⁵, Marina Serra^{5,6}, Giovanni Mario Pes², Denise Schloesser⁷, Elena Pizzuto⁴, Heiko Siegmund⁵, Claudia Fischer⁵, Anna Saborowski⁷, Gianluigi Giannelli⁴, Matthias Evert⁵, Luc Johannes Wilhelmus van der Laan¹, Monique Maria Andrea Verstegen¹, Diego Francesco Calvisi^{2,*}

JHEP Reports 2025. vol. 7 | 1–12



Background & aims: Intrahepatic cholangiocarcinoma (iCCA) is the second most frequent primary liver tumor, characterized by clinical aggressiveness, dismal outcome, and limited therapeutic options. Thus, innovative treatments are urgently required to improve the prognosis of patients with iCCA.

Methods: In this study, we determined the pathogenetic and therapeutic role of eukaryotic initiation factor 4A1 (EIF4A1), a subunit of the eIF4F complex involved in translation initiation, in human iCCA.

Results: Preinvasive (n = 12), invasive (n = 162), and metastatic (n = 14) iCCA lesions exhibited ubiquitous eIF4A1 upregulation. In addition, *eIF4A1* mRNA levels from 42 specimens showed a significantly higher expression in iCCA samples compared with non-tumorous tissues ($p < 0.0001$) or large duct-type lesions ($p = 0.020$). Furthermore, *eIF4A1* expression was inversely associated with patient prognosis ($p < 0.001$). Moreover, zotatifin, an eIF4A1-specific inhibitor in clinical trials, significantly reduced the growth of iCCA cell lines, iCCA cancer-associated fibroblasts (CAFs), and patient-derived tumor organoids. At the metabolic level, zotatifin decreased glycolysis of iCCA cells without affecting mitochondrial respiration. Moreover, the Bcl-xl inhibitors A-1155463 and DT2216 profoundly augmented apoptotic cell death when administered in association with zotatifin.

Conclusions: The data highlight eIF4A1 as a potential target for treating iCCA. Combined inhibition of eIF4A1 and Bcl-xl could offer an effective therapeutic strategy against this deadly disease.

© 2025 The Author(s). Published by Elsevier B.V. on behalf of European Association for the Study of the Liver (EASL). This is an open access article under the CC BY-NC-ND license (<http://creativecommons.org/licenses/by-nc-nd/4.0/>).

Introduction

Intrahepatic cholangiocarcinoma (iCCA) is an aggressive form of liver cancer associated with poor prognosis and limited therapeutic options. In most cases, iCCA is diagnosed at a late stage, which limits curative treatments, such as surgical resection, and leaves chemotherapy, combining gemcitabine and platinum-derived drugs, as the primary option.^{1,2} Epidemiological studies have highlighted the constant rise in the incidence and mortality of iCCA in the USA and Europe. Furthermore, data from the American Cancer Society and the Surveillance, Epidemiology, and End Results (SEER) program indicate that the 5-year survival rate for intrahepatic bile duct cancer is ~9%.^{3,4}

In this gloomy scenario, the US FDA and the EMA recently approved the use of personalized therapies.^{5–8} However, their efficacy is often temporary because drug resistance ultimately develops as a result of tumor heterogeneity and tumor cell plasticity.⁹ Therefore, it is vital to identify novel therapeutic vulnerabilities and treatments to significantly improve the prognosis and management of patients with iCCA.

Translation initiation is the rate-limiting step in protein synthesis, and its targeted inhibition is emerging as a promising

approach for cancer treatment.¹⁰ Indeed, in cancer cells, different oncogenic signaling pathways rewire the translation machinery to support tumorigenesis via aberrant proliferation, survival, metastasis, and chemoresistance.¹¹ Multiple eukaryotic initiation factors (eIFs) participate in translation initiation, with the cap-binding complex eukaryotic initiation factor 4F (eIF4F) being a key component.¹² The eIF4F complex primarily comprises three constituents, eIF4E, eIF4G, and eIF4A, which induce cap-dependent ribosome recruitment and translation initiation. eIF4A is the only component of the complex with enzymatic activity, namely an RNA helicase that facilitates ribosome scanning of mRNAs.¹³ Multiple oncogenes that contain structured 5'-untranslated regions (UTRs) require eIF4A activity for translation, such as KRAS, MYC, BCL2, NOTCH1, HSF1, CDK6, and CCND1.^{14–17}

eIF4A has become an attractive therapeutic target, and several inhibitors targeting its helicase function have been developed. A family of inhibitors isolated from *Aglaia* species, known as rocaglates, including different natural molecules, such as silvestrol and rocaglamide A,¹⁸ exhibit antitumor activity by clamping eIF4A onto mRNA polypurine sequences, preventing its incorporation into the eIF4F complex.¹⁹ This

* Corresponding author. Address: Department of Medicine, Surgery, and Pharmacy, via P. Manzella 4, 07100 Sassari, Italy. Tel.: +39 079 228356. E-mail address: calvisid@uniss.it (D.F. Calvisi). <https://doi.org/10.1016/j.jhepr.2025.101416>



induces translation repression and translome remodeling by blocking ribosome scanning of the pre-initiation complex and other mechanisms.^{19,20}

eIF4A1 overexpression occurs in various cancer types and is associated with invasion and poor prognosis, further suggesting the therapeutic potential of rocaglates.^{21–26} In addition, several synthetic rocaglate derivatives have been generated to enhance the drug properties of the natural compounds. Among these drugs, zotatifin (eFT226) showed improved drug-like properties and is the first-in-class eIF4A inhibitor.²⁷

Here, we investigated the levels of eIF4A1 in iCCA specimens from patients and the efficacy of zotatifin in numerous *in vitro* models of iCCA. Our data indicate targeting eIF4A with zotatifin as a promising therapeutic approach for this tumor type.

Materials and methods

Human tissue specimens

In total, 198 iCCA tissue samples from surgical resections were collected and underwent histopathological analysis by certified expert pathologists at the Institute of Pathology of the University of Regensburg (Regensburg, Germany). The study followed the guidelines of the Declaration of Helsinki and was approved by the Clinical Research Ethics Committee of the Medical University of Regensburg (protocol code 17-1015-101). Informed consent was obtained from all individuals. The Medical Ethical Council of the Erasmus MC approved the use of tumor tissue for organoid initiation, and written informed consent was again provided by all patients (MEC-2013-143). Human intrahepatic cancer-associated fibroblasts (hCAFs) were collected and used following approval by the Ethical Committees from the Azienda Ospedaliero Universitaria Consorziale Policlinico di Bari (Bari, Italy; protocol number: 254). Informed consent was obtained from all individuals.

Table S1 summarizes patients' clinicopathological features.

Initiation, propagation, and validation of iCCA organoids

The iCCA organoids (iCCAOs) used in this study, referred to as iCCAO1 and iCCAO2, were derived from tumor samples from patients CCA2 and CCA3, respectively, as described by Broutier *et al.*²⁸ These organoids were established and validated in the original study, where they were shown to retain the histological and molecular features of the parental tumors.

Cell lines and reagents

HUCCT1, CCLP1, KCU-M213, KCU-M156, KCU055, SG231, and RBE human iCCA cells, purchased from the Japanese Collection of Research Bioresources (JCRB; Ibaraki, Osaka, Japan) or the American Type Culture Collection (ATCC; Manassas, VA, USA), were used for the experiments. These cell lines display a wide spectrum of mutations occurring in human iCCA (Table S2).³¹

Human cancer-associated fibroblast (CAF) isolation and treatment

Human intrahepatic cancer-associated fibroblasts (hCAFs) were collected and used following the approval by the Ethical Committees from the Azienda Ospedaliero Universitaria

Consorziale Policlinico di Bari (Bari, Italy; protocol number: 254, 2012).

Statistical analysis

GraphPad Prism version 10.2.1 software and IBM SPSS version 26 software (IBM, Armonk, NY, USA) were used to analyze the data for statistical significance.

Additional Materials and methods are available in the Supplementary Data.

Results

eIF4A1 is overexpressed in human intrahepatic cholangiocarcinoma

First, we analyzed the mRNA levels of *eIF4A1* in iCCA samples from patients and their corresponding non-tumorous adjacent liver tissues. In total, 42 samples were collected at the University of Regensburg, with both frozen tissues and patients' survival data available for analysis. Quantitative real-time RT-PCR analysis showed that *eIF4A1* mRNA expression was significantly higher in iCCA specimens than in paired non-tumorous tissues ($p < 0.0001$; Fig. 1A). In addition, *eIF4A1* levels were significantly higher in large duct-type iCCA specimens compared with small duct type ($p = 0.020$) and mixed ($p = 0.028$) lesions (Fig. 1B). Notably, when assessing the prognostic relevance of the gene, *eIF4A1* levels were inversely associated with patient survival time ($p < 0.001$; Fig. 1C). Furthermore, univariate analysis revealed a significant difference in survival for lymph node metastasis, lung metastasis, histology, and *eIF4A1* expression (Supplementary Material). Moreover, multivariate analysis showed a significant difference in *eIF4A1* levels in terms of survival, lymph node metastasis, lung metastasis, and histology (Supplementary Material). In addition, we determined the proliferation rate of all iCCA samples tested and found that the Ki-67 index directly and significantly correlated with *eIF4A1* levels ($r = 0.752$; $p < 0.0001$) (Fig. 1D). Similar data were obtained when analyzing *eIF4A1* expression in the iCCA data extracted from The Cancer Genome Atlas (TCGA) database (Fig. S1).

Subsequently, we evaluated the immunohistochemical pattern of eIF4A1 in a larger sample collection. In normal livers ($n = 10$), hepatocytes and cholangiocytes exhibited faint to moderate cytoplasmic eIF4A1 immunolabeling (Fig. S2A). By contrast, pronounced cytoplasmic eIF4A1 immunoreactivity characterized preinvasive lesions ($n = 12$, comprising six intraductal papillary biliary neoplasms [IPBN] and six biliary epithelial neoplasias [BiIIN]; Fig. S2B). Similarly, iCCA lesions ($n = 162$) showed robust eIF4A1 immunoreactivity, which demarcated the tumors from the non-neoplastic surrounding tissues (Fig. 2A,B). Furthermore, iCCA metastases ($n = 14$, comprising six lymph node metastases and eight peritoneal metastases) exhibited strong cytoplasmic accumulation of eIF4A1 (Fig. 2C).

In addition, we evaluated whether eIF4A1 immunohistochemistry was related to a specific histological subtype. In our sample collection, 92 of 162 (56.8%) iCCA samples were of the small duct type, 60/162 (37.3%) were of the large duct type, and the remaining 10/162 (6.2%) displayed features of both types and were referred to as 'mixed'. eIF4A1 levels were ubiquitously upregulated in iCCA lesions, with a slightly stronger immunoreactivity in large duct type iCCA (Fig. S3).

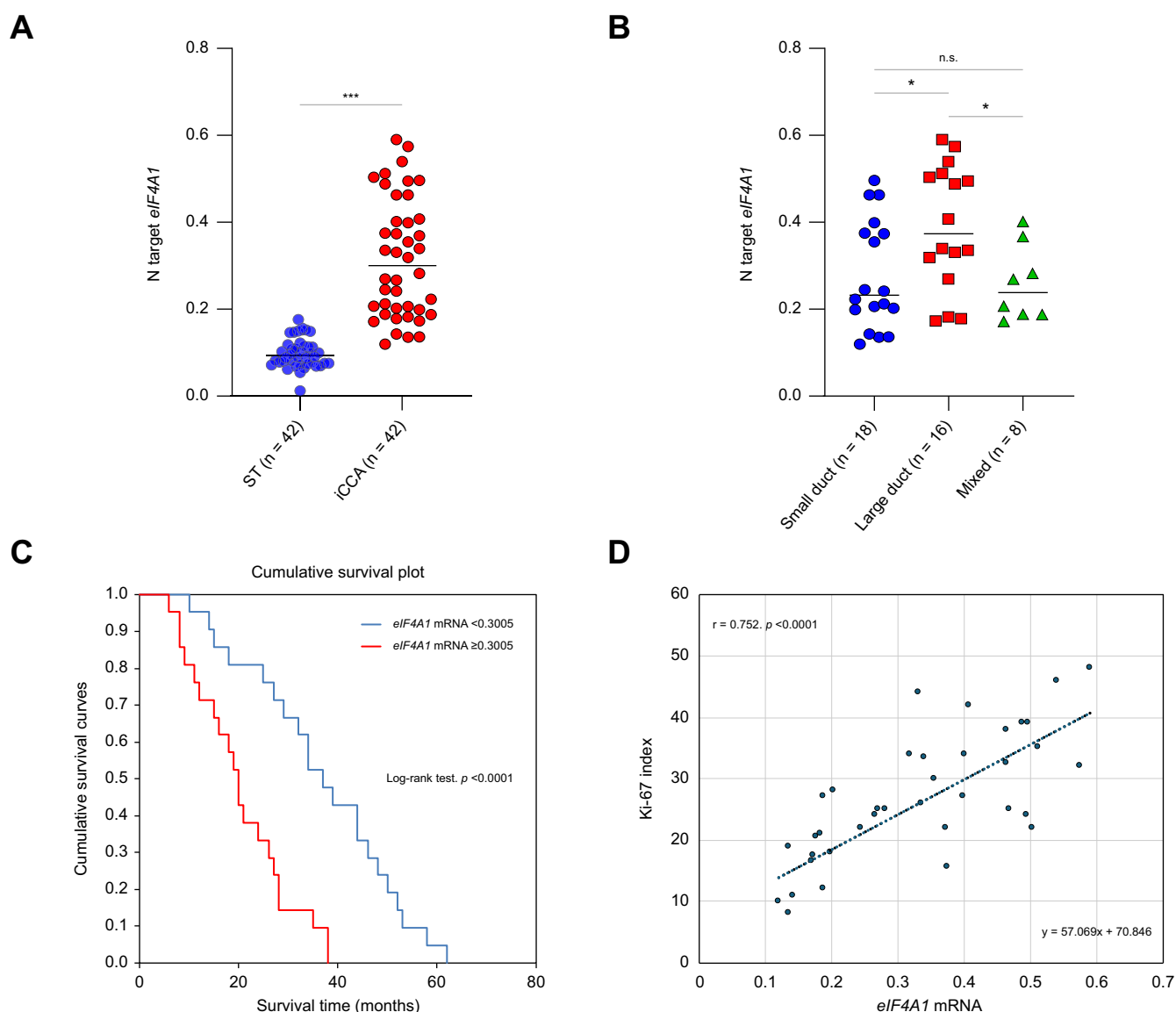


Fig. 1. eIF4A1 is upregulated in human iCCA specimens. (A) Quantitative real-time RT-PCR values of *eIF4A1* were significantly higher in T (n = 42) compared with corresponding non-tumorous ST. Student's *t* test: *** $p < 0.0001$. (B) *eIF4A1* levels were significantly higher in large duct-type iCCA than in small duct and mixed iCCA. Tukey's multiple comparisons test: * $p < 0.05$; N.S., not significant. (C) Kaplan-Meier curve showing that *eIF4A1* mRNA levels negatively correlated with patient survival. (D) Linear regression analysis revealing that *eIF4A1* mRNA expression directly correlated with tumor proliferation (as assessed by Ki-67 index) in iCCA samples. *eIF4A1*, eukaryotic initiation factor 4A1; iCCA, intrahepatic cholangiocarcinoma; ST, surrounding tissue; T, tumorous tissue.

Overall, the present data reveal the upregulation of *eIF4A1* in iCCA development and progression.

Targeting *eIF4A1* with zotatifin restrains cell growth in iCCA cells and downregulates the E2F1 pathway

Next, to determine the cytotoxic potential of targeting *eIF4A1* activity in iCCA, we administered the *eIF4A1* specific-inhibitor zotatifin to seven human iCCA cell lines (RBE, HUCCT1, CCLP1, KKU-M213, KKU-M156, KKU055, and SG231). Zotatifin was chosen because it is the only *eIF4A* inhibitor undergoing clinical trials. Zotatifin profoundly reduced tumor cell viability in the cell lines tested in a dose-dependent manner (Fig. 3A). In all cell lines, the calculated half-maximal inhibitory concentration (IC_{50}) values for zotatifin were in the low

nanomolar range. Zotatifin administration was similarly detrimental for the growth of four additional murine iCCA-derived cell lines harboring some of the most frequent mutations in this disease (p53 loss, IDH1^{R132H}, FGFR2 fusion, KRAS^{G12D}, and BRAF^{V600E}) (Table S3).³²

To clarify the mechanisms of action of zotatifin in iCCA cell lines, we randomly selected four cell lines (RBE, HUCCT1, KKU-M213, and KKU-M156) for the following experiments. In terms of cell proliferation, incubation with 15 nM Zotatifin (a concentration around its IC_{50} value) caused a similar, remarkable reduction in BrdU incorporation in the cell lines (Fig. 3B–E). Concerning apoptosis, zotatifin induced higher apoptotic cell death in RBE, HUCCT1, KKU-M213, and KKU-M156 cell lines than in untreated and DMSO-treated cells (Fig. S4A–D).

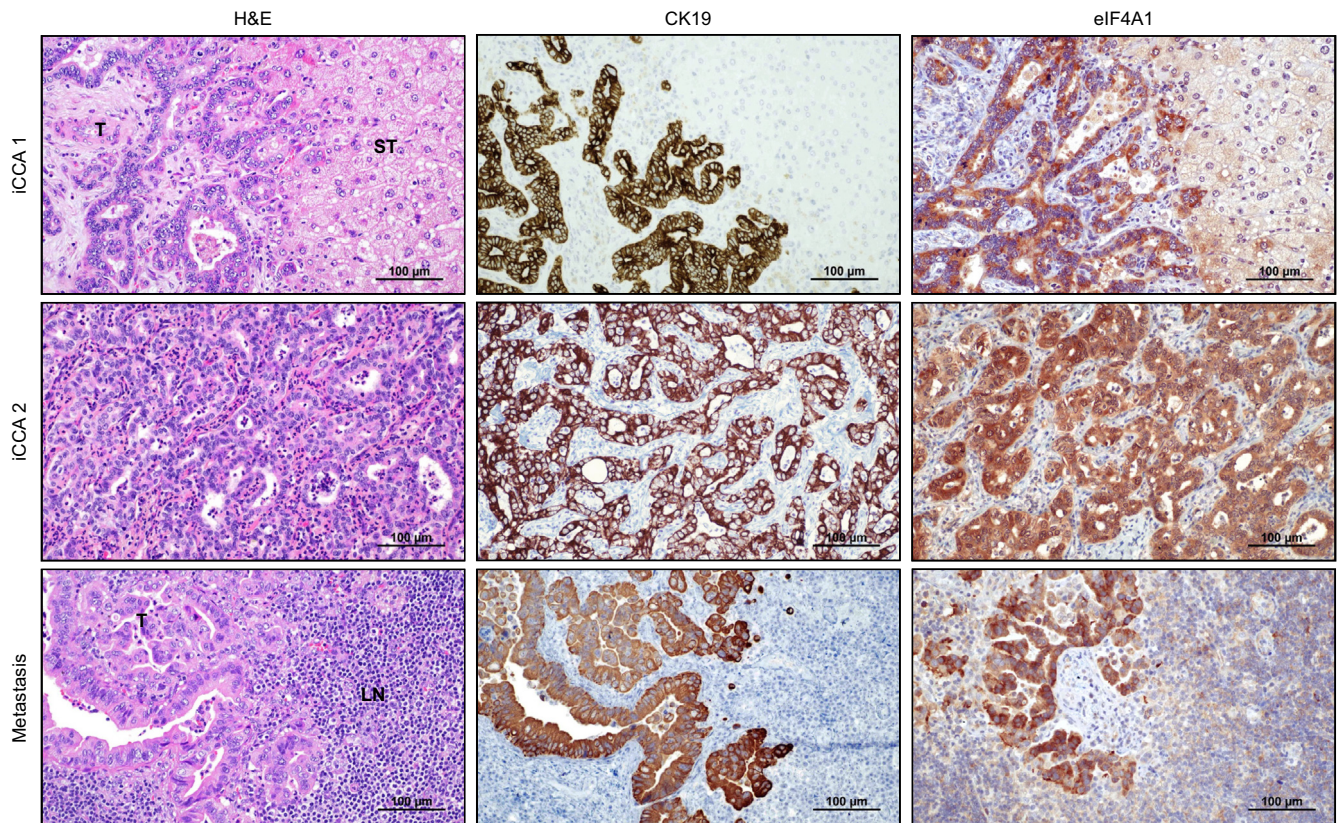


Fig. 2. Representative eIF4A1 immunohistochemistry patterns in human invasive iCCA and metastatic lesions. Top panels: example of human invasive iCCA (denominated iCCA1). There was enhanced immunoreactivity for eIF4A1 in T compared with neighboring non-tumorous ST, which exhibited faint/moderate eIF4A1 staining. Middle panels: staining features of eIF4A1 protein in an invasive iCCA (denominated iCCA2). The lesion exhibited robust cytoplasmic immunolabeling for eIF4A1. Lower panels: an iCCA LN metastasis displaying pronounced eIF4A1 cytoplasmic immunoreactivity. The LN and T tissues of the specimen showed moderate and intense immunolabeling for eIF4A1, respectively. CK19 staining was used as a biliary marker. Scale bars: 100 μm. eIF4A1, eukaryotic initiation factor 4A1; iCCA, intrahepatic cholangiocarcinoma; LN, lymph node; ST, surrounding tissue; T, tumorous tissue.

To substantiate our findings, HUCCT1 and KKKU-M213 cell lines were treated with zotatifin and flow cytometry analysis was performed. Zotatifin caused a substantial increase in cell apoptosis in a dose-dependent manner compared with the vehicle (Fig. 4A,B; Fig. S5A and B). Cell cycle analysis was then performed to evaluate the effects of zotatifin on cell cycle phase distribution in the same cell lines. Treatment with zotatifin compared with vehicle affected predominantly the G1/S transition of the cell cycle, with an obvious accumulation in the S phase (Fig. 4C,D; Fig. S5C and D). Similar effects in terms of apoptosis and cell cycle following Zotatifin administration were obtained in KKKU-M156 cells (not shown).

Subsequently, we investigated the molecular mechanisms whereby zotatifin perturbs cell cycle progression in iCCA cells. Specifically, we focused on the E2F1 transcription factor, a major player in G1/S transition and cell cycle progression.³³ Notably, zotatifin administration to KKKU-M213 and HUCCT1 cell lines significantly reduced the mRNA levels of the *MKI67* and *PCNA* proliferation markers and *E2F1* and its canonical targets involved in cell cycle progression (*FOXM1*, *SKP2*, *MCM2*, *MCM7*, *CYCLIN D1*, *RRM2*, and *MYBL2*). Furthermore, zotatifin decreased the levels of E2F1 targets involved in purine (*ATIC*, *GMPS*, and *GFAS*) and pyrimidine (*CAD*) metabolism, which serve as building blocks for DNA and RNA, promoting cell survival and proliferation (Fig. S6).

These data indicate that zotatifin potently suppresses the growth of iCCA cell lines regardless of the driving mutations, possibly by perturbing cell cycle progression and inhibiting the E2F1 pathway.

Zotatifin decreases glycolysis and triggers glutaminolysis in iCCA cells

To evaluate whether zotatifin affects iCCA metabolism, we assessed its influence on mitochondrial respiration and glycolysis of HUCCT1 and KKKU-M156 cells. The oxygen consumption rate was quantified to determine the mitochondrial respiratory capacity (Fig. 5A,B). Zotatifin did not limit the maximal respiration rate of either cell line. In accordance, transmission electron microscopy showed the absence of mitochondrial alterations in HUCCT1 cells following zotatifin treatment (Fig. S7). Indeed, no changes in number, perimeter, size, sphericity, morphology of the cristae and membranes, or elongation/condensation of mitochondria occurred in zotatifin-treated HUCCT1 cells compared with DMSO-treated cells. By contrast, zotatifin drastically decreased the basal and compensatory glycolytic capacity in HUCCT1 and KKKU-M156 cells (Fig. 5C,D).

Subsequently, we investigated the effect of zotatifin administration on the levels of metabolism players in HUCCT1

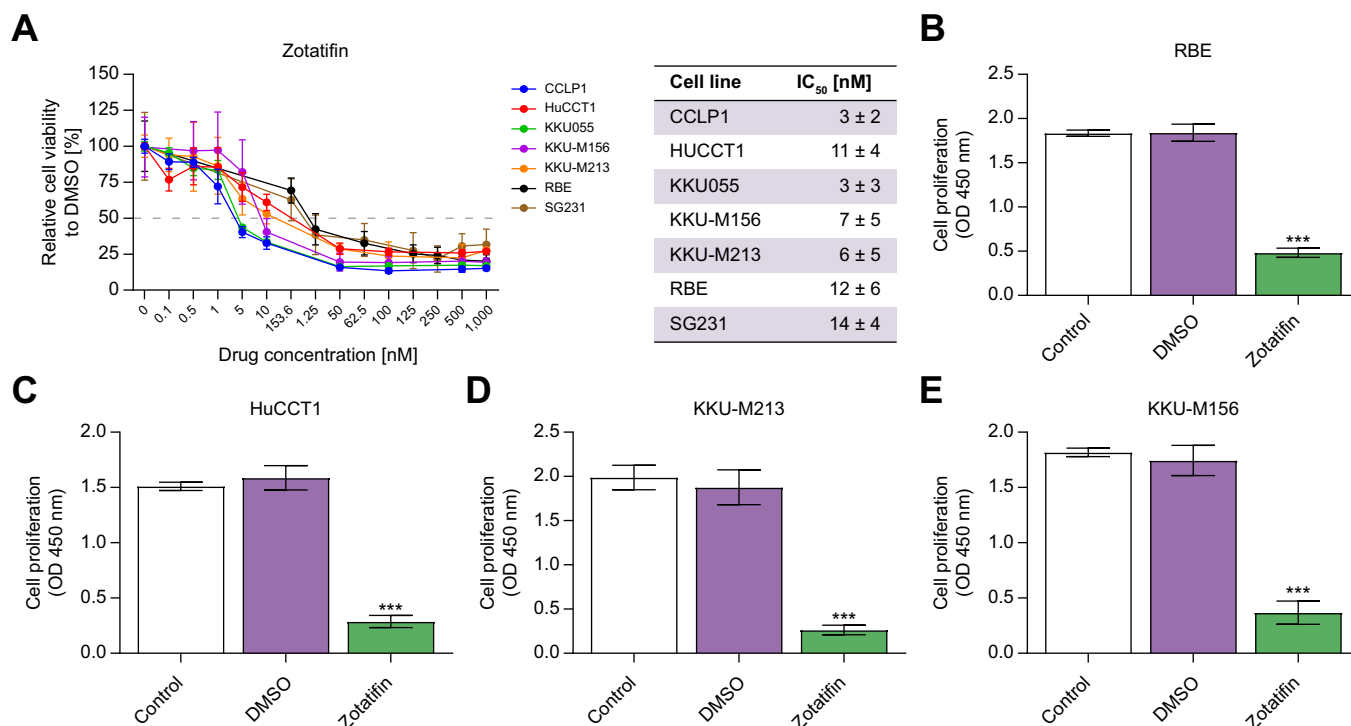


Fig. 3. The eIF4A inhibitor zotatifin negatively effects the growth of iCCA cell lines. (A) Cell viability of seven human iCCA cell lines (CCLP1, HUCCT1, KKU055, KKU-M156, KKU-M213, RBE, and SG231) exposed to zotatifin as assessed by MTT assay. Data are the percentage of DMSO-treated cells ± SD; n = 3. The IC₅₀ ± SD of zotatifin in each cell line is also provided. (B–E) A BrdU incorporation assay was conducted on (B) RBE, (C) HUCCT1, (D) KKU-M213, and (E) KKU-M156 cells treated for 48 h with 15 nM zotatifin. Untreated cells and cells treated with DMSO served as controls. Data are mean ± SD; n = 3; analyzed using Tukey's multiple comparisons test; ***p < 0.0001 vs. control and vs. DMSO. eIF4A1, eukaryotic initiation factor 4A1; iCCA, intrahepatic cholangiocarcinoma; OD, optical density.

and KKU-M156 cells (Fig. S8). Zotatifin downregulated several glycolysis-related genes (*ALDOC*, *PFKFB1*, *PGAM1*, and *LDHA*) in the two cell lines, suggesting that zotatifin modulates glycolysis at several levels. Similar results were detected in KKU-M213 cells treated with Zotatifin (not shown). By contrast, zotatifin induced the upregulation of *GLS1*, a pivotal player in glutaminolysis, and the *c-Myc* transcription factor. Given that the upregulation of glutaminolysis has been identified as a mechanism of resistance to eIF4A1 inhibition in pancreatic cancer cells,¹⁵ we treated the KKU-M156 and HUCCT1 cell lines with zotatifin either alone or in association with the *GLS1* inhibitor telaglenastat. The combination of zotatifin (15 nM) and telaglenastat (2 μM) resulted in a significantly higher reduction of proliferation and more robust apoptosis in the two cell lines compared with either treatment administered alone (Fig. S9).

These data indicate that zotatifin does not affect mitochondrial respiration, hampers glycolysis, and induces glutaminolysis in iCCA cells.

Combining zotatifin and Bcl-xl inhibitors restrains the growth of iCCAOs *in vitro*

To further elucidate the therapeutic role of zotatifin in iCCA, we assessed its effects in iCCAOs. We exposed two iCCAOs (iCCA01 and iCCA02)^{28–30} to increasing concentrations of zotatifin and assessed the cell viability after 48 h (Fig. 6A). The results demonstrated a gradual decrease in cell viability in the two iCCAOs as the concentration of zotatifin increased. At a low concentration of zotatifin (50 nM), cell viability in the

organoids decreased to 57–78%. When the concentration was increased 200-fold to 10,000 nM, cell viability decreased to 31–55%. This suggests that higher concentrations of zotatifin have a diminishing effect on iCCA0 viability. Microscopic observations revealed morphological changes in iCCA0s after 48 h of treatment with 1,000 nM Zotatifin (Fig. 6B). Changes included substantial shrinkage, collapse, and solidification of the organoids. However, there was no obvious evidence of extensive cell death, such as widespread dark organoid debris, and only scattered fragments of organoids were observed. Consequently, we explored combination treatments. To increase cell death, we tested the combination of zotatifin with the Bcl-xl inhibitors A-1155463 (1 μM) or DT2216 (10 μM) (Fig. 6C–E). After 48 h of treatment, the two iCCA0s lines showed significant synergistic effects (p < 0.05), confirming the potential efficacy of this combination therapy.

Bcl-xl inhibitors enhance apoptosis in combination with zotatifin in iCCAOs

Next, we performed Calcein AM and propidium iodide (PI) staining assays to confirm that combining zotatifin with Bcl-xl inhibitors leads to increased cell death (Fig. 7). Compared with the control group, administration of the Bcl-xl inhibitor A-1155463 (1 μM) alone resulted in a few organoid fragments stained red by PI, indicating cell death. However, most organoids maintained their complete and healthy morphology, similar to the control group. In the zotatifin (1 μM)-only group, although the organoid morphology changed (shrinkage,

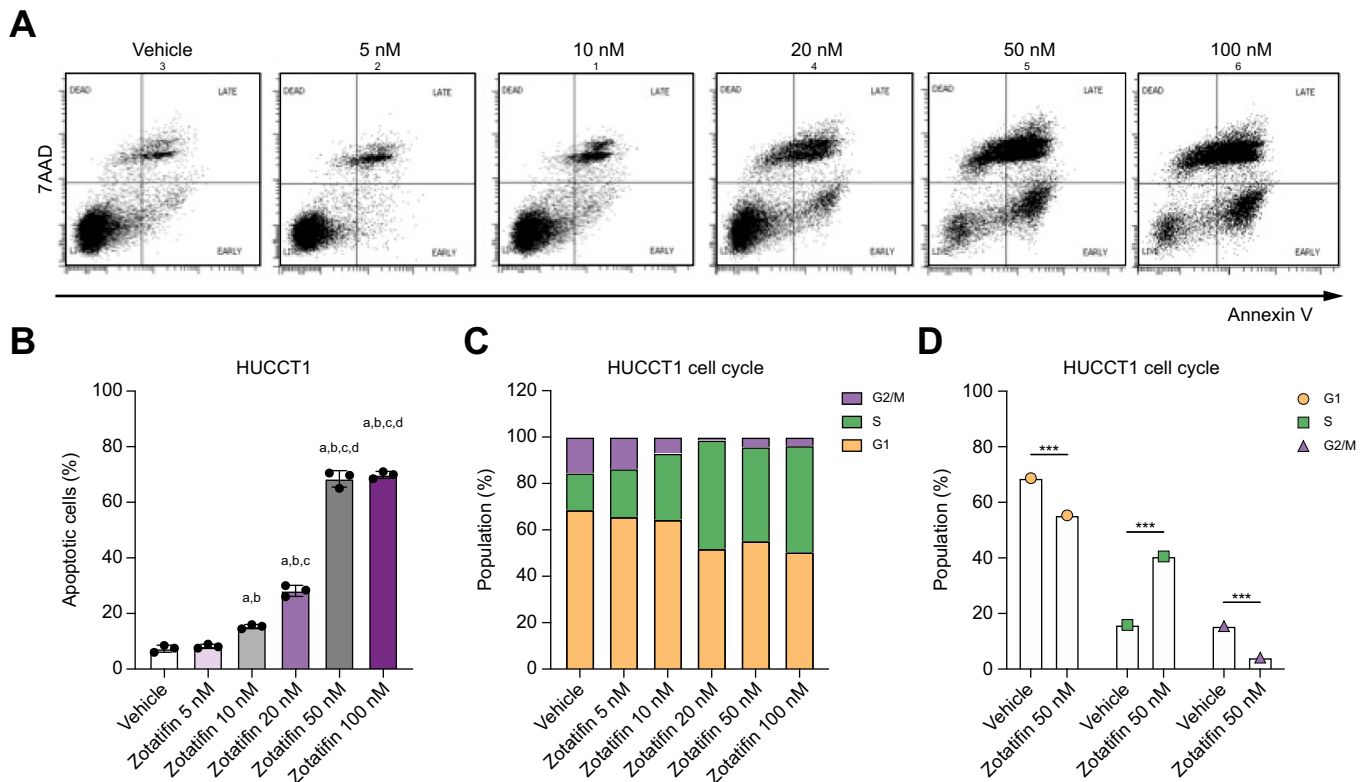


Fig. 4. Effect of the eIF4A inhibitor zotatifin on the apoptosis and cell cycle of iCCA cell lines, as assessed by flow cytometry analysis. (A,B) Apoptotic analysis with Annexin V-PE and 7-AAD staining of HUCCT1 iCCA cells treated with different concentrations of zotatifin for 48 h. Data are mean \pm SD percentage of total apoptotic cells; $n = 3$; analyzed using ANOVA: $***p < 0.001$ according to Tukey's multiple comparisons test. Lowercase letters denote statistical significance (a, vs. vehicle; b, vs. zotatifin 5 nM; c, vs. zotatifin 10 nM; d, vs. zotatifin 20 nM). (C) Representative images of the cell cycle distribution of HUCCT1 iCCA cells cultured in the presence of different concentrations of zotatifin for 48 h. (D) Quantification of the cell cycle phases comparing vehicle with zotatifin 50 nM. Data are mean \pm SD; $n = 3$; analyzed using a two-tailed, unpaired Student's t test; $***p < 0.001$. eIF4A1, eukaryotic initiation factor 4A1; iCCA, intrahepatic cholangiocarcinoma.

collapse, and solidification), these organoids were stained green by Calcein AM, indicating they were still viable. Only a few cell fragments around the organoids were stained red by PI. These results suggest that neither zotatifin nor Bcl-x1 inhibitors alone induce widespread cell death in iCCAOs.

By contrast, the combination treatment group showed that most organoids had shrunk significantly, with many fragments visible in and around the organoids in bright field images. These fragments were stained red by PI, indicating dead cells. This combination treatment induced more cell death compared with the single treatments. To further validate that this synergistic effect is mediated by inducing greater apoptosis, we compared the expression levels of the apoptosis-related protein cleaved caspase 3 before and after treatment (Fig. 8). The results indicated that single treatments with zotatifin (1 μ M) or A-1155463 (1 μ M) induced cleaved caspase 3 in only a small fraction of cells, with relatively intact organoid structures. However, over 40% of cells under combined treatment exhibited clear apoptotic signals ($p < 0.05$), and the organoid structures were disrupted, with numerous cell fragments scattered within and around the organoids. Similar results were observed in formalin-fixed and paraffin-embedded iCCAO samples (Fig. S10). Thus, the synergistic action of zotatifin and Bcl-x1 inhibitors in CCAOs results from the robust induction of apoptosis.

Based on the intriguing findings from iCCAOs, we determined whether the combination of zotatifin and Bcl-x1 inhibitor was also effective in human iCCA cell lines. When zotatifin (15 nM) was combined with DT2216 (1 μ M), a slight additive antiproliferative effect was observed only in K KU-M156 cells (Fig. S11A and B) compared with zotatifin alone, whereas proliferation remained unaffected by DT2216 single administration. Strikingly, massive apoptosis was induced in HUCCT1 and K KU-M156 cells when the two drugs were combined (Fig. S11C and D), thus recapitulating the iCCAO findings. At the molecular level, zotatifin treatment resulted in the induction of eIF4A1 and eIF4A2, established surrogate markers of eIF4A1 activity inhibition. Furthermore, the downregulation of prohibitin 1 (PHB1), a canonical target of eIF4A inhibitors, was observed. By contrast, DT2216 administration triggered the downregulation of its target Bcl-x1 and induction of the apoptosis marker cleaved PARP (Fig. S11E).

Zotatifin blunts CAF growth *in vitro*

Next, because mounting evidence from other tumor types suggests a role of eIF4A1 in regulating the tumor microenvironment,³⁴ we investigated the effect of zotatifin on the growth of human iCCA hCAFs. Immunohistochemistry of patient specimens revealed that eIF4A1 was highly expressed in the

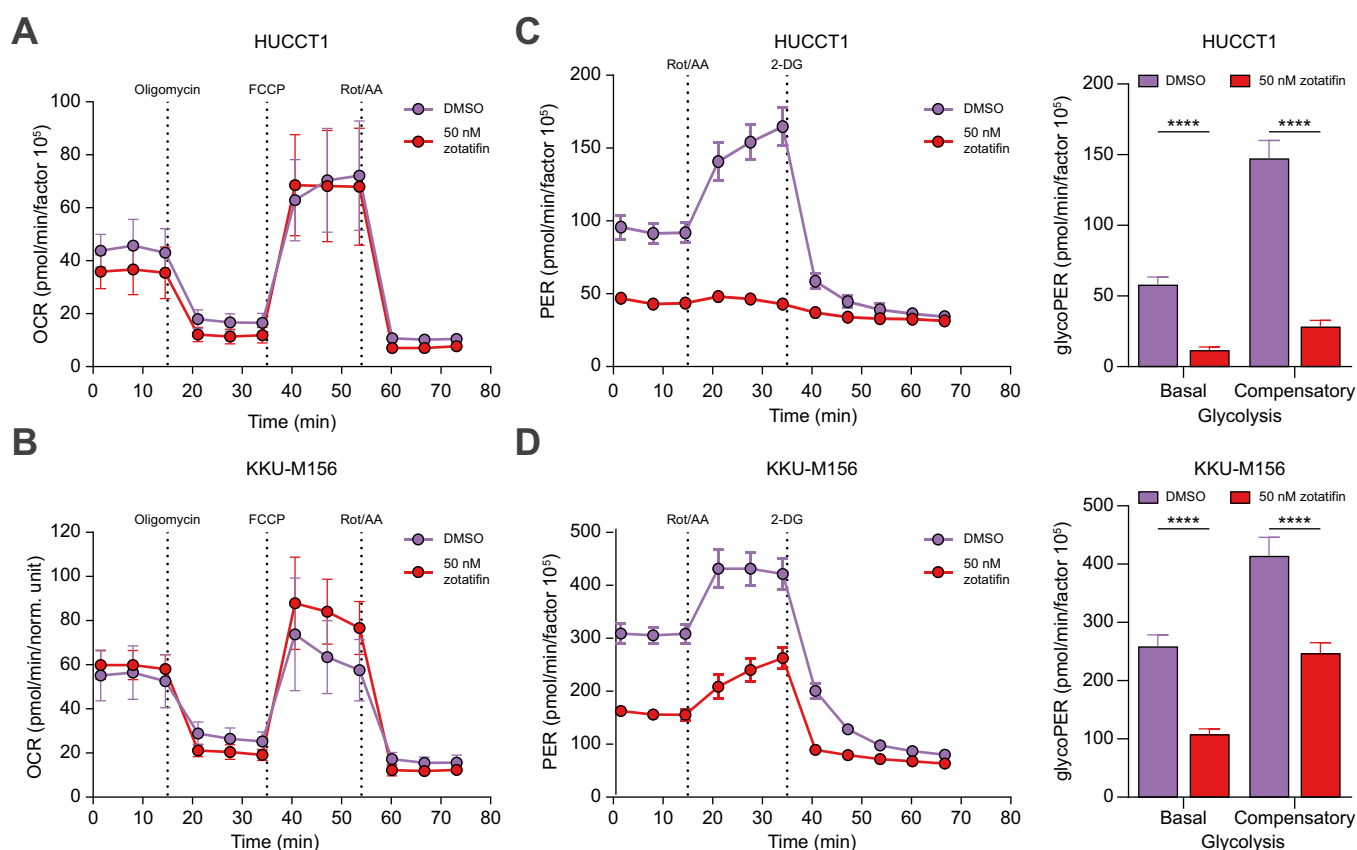


Fig. 5. Effect of the eIF4A1 inhibitor zotatifin on mitochondrial respiration and glycolysis in human iCCA cell lines. (A,B) Normalized OCR profile, as revealed by the Seahorse XF Mito Stress Test, in (A) HUCCT1 and (B) KKKU-M156 cells treated with 50 nM zotatifin or matched DMSO concentration for 24 h. All OCR levels were background corrected and normalized to nuclei fluorescent staining. Data are mean \pm SD; $n = 2$ (with technical triplicates). (C,D) For the Seahorse XF Glycolytic Rate Assay, (C) HUCCT1 and (D) KKKU-M156 cells were treated with 50 nM zotatifin or matched DMSO concentration for 24 h. ECAR and oxidative stress rates (OCR) were measured in the Seahorse XF HS mini analyzer and converted to PER using WAVE Pro. The first three measurements show basal respiration, followed by injection of Rot/AA and 2-DG after the third and sixth measurement, respectively. Data are mean \pm SD; $n = 2$. Right: Measures of basal and compensatory glycolysis calculated from the OCR traces in (C,D). Data are mean \pm SD; $n = 2$; analyzed with Tukey's multiple comparisons test; **** $p < 0.001$. Dotted lines indicate the time-point of compound injection. 2-DG, 2-deoxy-D-glucose; AA, antimycin A; ECAR, extracellular acidification rate; eIF4A1, eukaryotic initiation factor 4A1; FCCP, carbonyl cyanide- p -trifluoromethoxyphenylhydrazone; iCCA, intrahepatic cholangiocarcinoma; OCR, oxidative consumption rate; PER, total proton efflux rate; Rot, rotenone.

CAFs within the desmoplastic stroma surrounding the tumor lesions (Fig. S12). Subsequently, eight different hCAF lines were subjected to western blot analysis. Notably, the levels of eIF4A1 in seven of eight hCAF lines were higher than those detected in the LX2 human hepatic stellate cell line used as a control (Fig. S13A). Subsequently, hCAFs isolated from three distinct patients were administered various concentrations of zotatifin. Treatment of CAFs with zotatifin triggered a decrease in proliferation *in vitro* in a dose-dependent manner (Fig. S13B). Thus, Zotatifin treatment significantly decreases the *in vitro* growth of iCCA hCAFs.

Discussion

iCCA is an aggressive tumor characterized by an increasing incidence, silent presentation, limited treatment options, and a high mortality rate.¹⁻⁴ Despite recent advances in understanding iCCA pathobiological features and identifying actionable molecular targets, a pressing need remains for more effective therapies against this deadly disease.²⁻⁹

In this investigation, we focused on mRNA translation dysregulation and related eIF4A1 overactivity, a common feature of cancer,^{10,11,31} in iCCA. Our study revealed that eIF4A1 levels

were upregulated from preinvasive lesions to metastatic tumors, implying that eIF4A1 is required for iCCA development and progression. Furthermore, eIF4A1 expression inversely correlated with the length of patient survival and directly with the proliferation rate in this disease. Thus, it is tempting to speculate that eIF4A1 contributes to the acquisition of a more aggressive phenotype by intrahepatic biliary tumors.

Similarly, elevated levels of eIF4A1 are associated with a worse outcome in breast, cervical, gastric, and pancreatic cancer patients.^{21-26,30} Therefore, our data substantiate the pathogenetic and prognostic importance of eIF4A1 in iCCA.

Moreover, *in vitro* approaches indicated that eIF4A1 inactivation by zotatifin was highly detrimental to the growth of various human and murine iCCA cell lines, irrespective of the driving mutations and CAFs. Therefore, eIF4A1 induction might not be restricted to a specific molecular iCCA subtype. Instead, it represents a ubiquitous event, a point of convergence for multiple oncogenic pathways to drive protein translation initiation in this disease. Notably, growth restraint of malignant cells and hCAFs was reached at low nanomolar concentrations of zotatifin, highlighting the potency of the drug, at least *in vitro*. Consequently, targeting eIF4A1 could impact the cancer cells and tumor microenvironment.

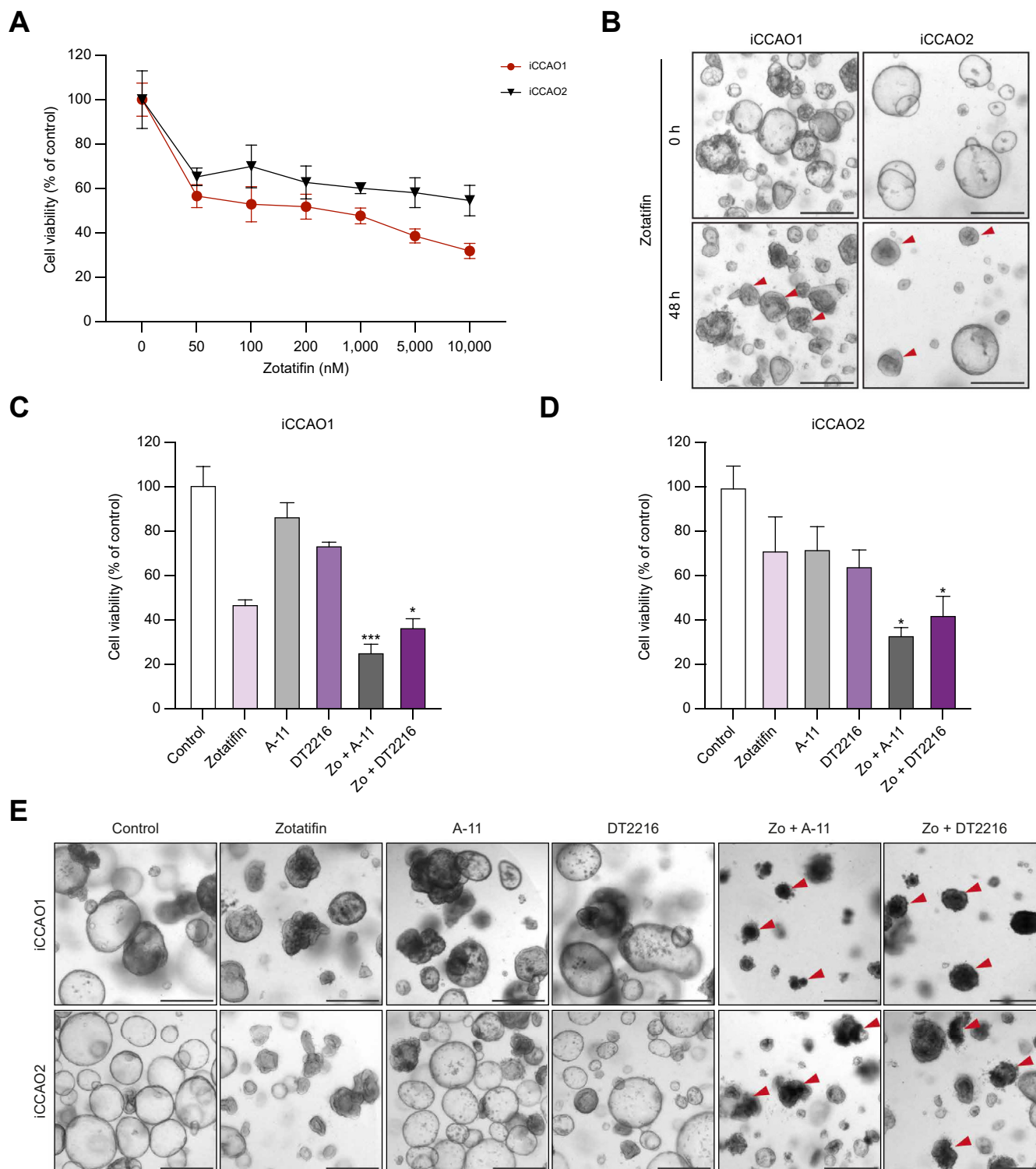


Fig. 6. Combining zotatfin and Bcl-x1 inhibitors restrains the growth of iCCAOs. (A) Cell viability of two iCCAOs cultured with increasing concentrations of zotatfin (0–10,000 nM) for 48 h, assessed using the CellTiter-Glo assay. (B) iCCAOs were treated with 1 μ M zotatfin for 48 h. Representative brightfield images from three independent experiments are shown. Arrowheads indicate iCCAOs with typical characteristics of shrinkage, collapse, and solidification. (C,D) Cell viability after 48 h of treatment with vehicle (DMSO), zotatfin 1 μ M alone, A-1155463 (A-11) 1 μ M alone, DT2216 10 μ M alone, and combination treatments of zotatfin with A-11 or DT2216, measured using the CellTiter-Glo assay. Data are mean \pm SD; n = 5; analyzed with unpaired two-tailed Student's t-test; * p < 0.05; *** p < 0.001; **** p < 0.0001. (E) Morphological changes in iCCAOs treated with zotatfin (1 μ M), A-11 (1 μ M), DT2216 (10 μ M), or a combination thereof, for 48 h. Arrowheads indicate fragmented iCCAOs. Scale bars: 500 μ m. iCCA0, intrahepatic cholangiocarcinoma organoid.

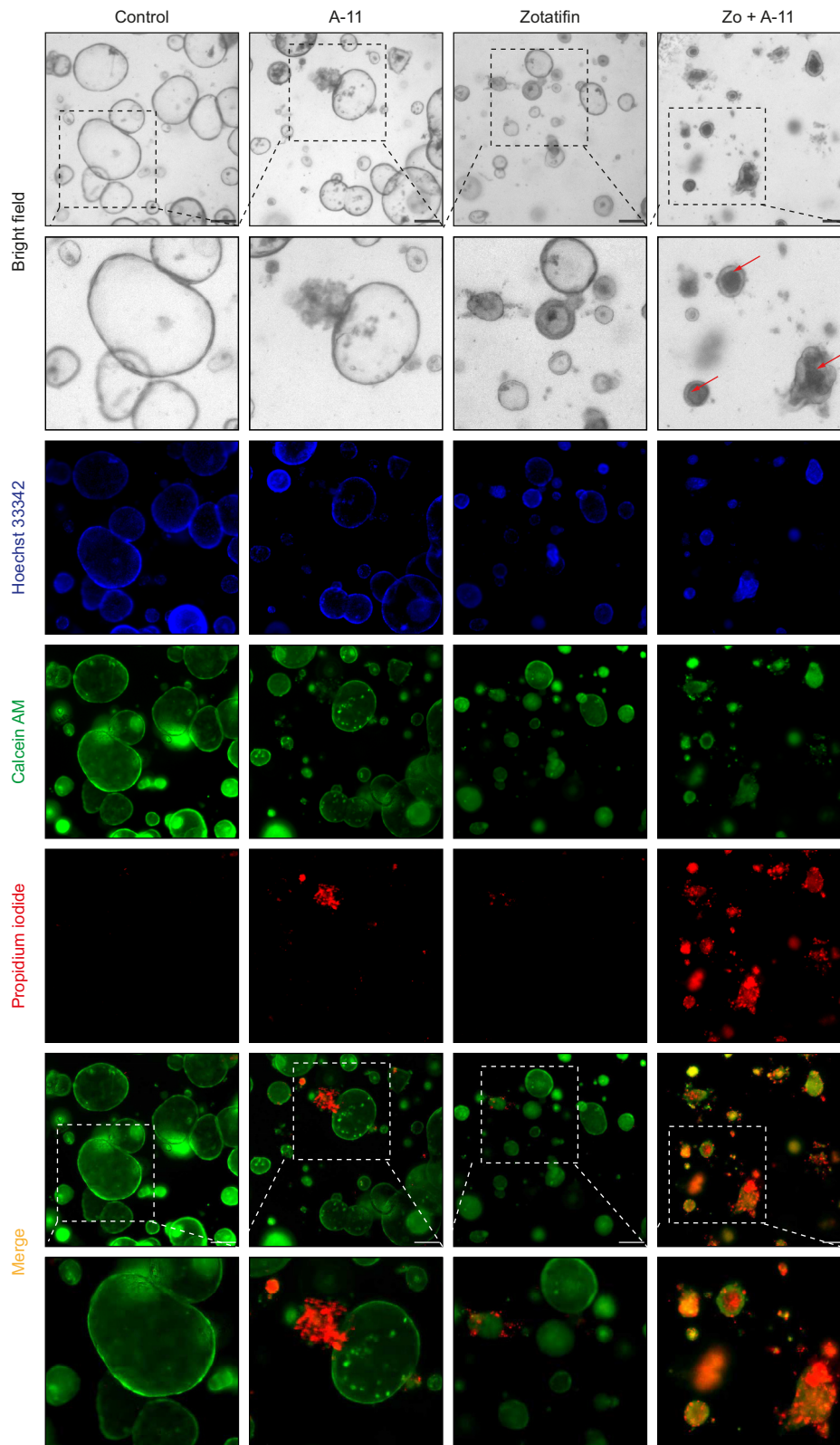


Fig. 7. The Bcl-xl inhibitor A-11 enhances cell death in combination with zotatifin in iCCAOs. Representative brightfield and fluorescence images of live–dead staining using Calcein AM (live, green), PI (dead, red), and Hoechst (nuclei, blue) for iCCAOs exposed to 1 μ M A-11, 1 μ M zotatifin, and a combination thereof for 48 h. Scale bars: 500 μ m. iCCAo, intrahepatic cholangiocarcinoma organoid; PI, propidium iodide.

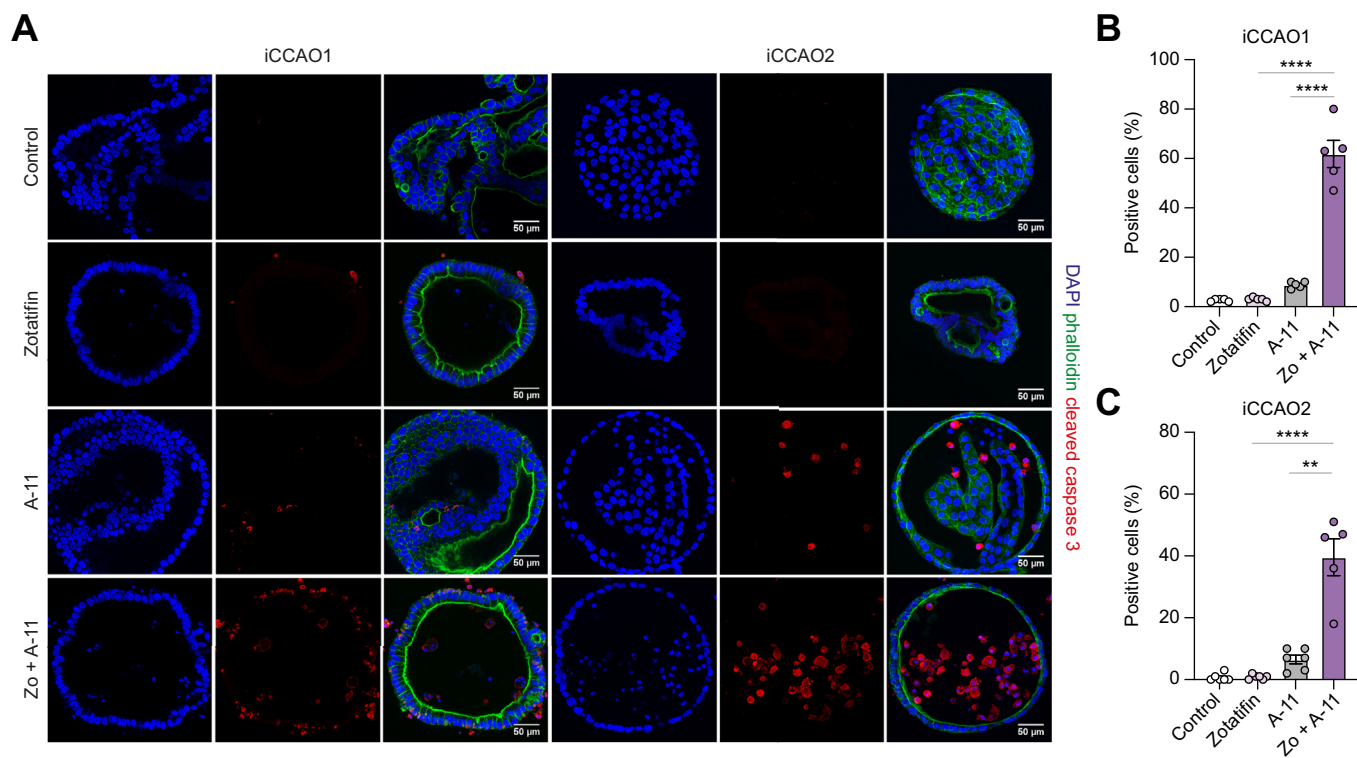


Fig. 8. The Bcl-x1 inhibitor A-11 enhances apoptosis in combination with zotatifin in iCCAOs. (A) Cleaved caspase 3 expression in iCCAOs after incubation with 1 μ M zotatifin, 1 μ M A-11, or a combination thereof. Images show cleaved caspase 3 staining (red), nuclear staining (DAPI, blue), and phalloidin staining (green) merged. (B–C) Quantification of positive cells from the images revealed significant differences in apoptotic cell populations among the different treatments. Data are mean \pm SD; n = 5; analyzed with unpaired two-tailed Student's t-test; ** p < 0.01; **** p < 0.0001. Scale bars: 50 μ m. iCCAo, intrahepatic cholangiocarcinoma organoid.

At the molecular level, the reduction in iCCA cell proliferation and cell cycle perturbation following zotatifin administration was paralleled by the suppression of the E2F1 transcription factor and its downstream effectors involved in cell cycle progression and purine and pyrimidine synthesis, unveiling E2F1 as a potentially critical target of zotatifin. Regarding metabolism, zotatifin treatment decreased glycolysis while inducing glutaminolysis in iCCA cells. Similar data were previously obtained in pancreatic adenocarcinoma cells.¹⁵ Notably, concomitant administration of zotatifin and the GLS1 inhibitor telaglenastat suppressed iCCA cell growth more profoundly compared with each treatment alone. This finding unravels glutaminolysis as a resistance mechanism exploited by tumor cells subjected to eIF4A inhibition and defines a novel therapeutic strategy to curb this metabolic compensation.

Interestingly, zotatifin exhibited a less pronounced cytotoxic effect in iCCAOs, yet it remained highly effective at inhibiting cell viability. For instance, brightfield microscopy, PI and Calcein AM staining, and immunofluorescence indicated that zotatifin did not markedly induce cell death in the organoids. This disparity might be the result of intrinsic differences between organoids and cell lines, such as the 3D architecture of organoids, which preserves cell–cell and cell–matrix interactions that provide survival and resistance signals. Based on these observations, we investigated combination therapies with other anticancer agents. Recent studies have emphasized

the crucial role of Bcl-x1 in regulating apoptosis.^{35–37} Bcl-x1 is a member of the Bcl-2 protein family, known for its role in preventing apoptosis and contributing to chemoresistance in various cancers.³⁸ Selective Bcl-x1 inhibitors, such as A-1155463 and DT2216, have been developed to overcome this resistance.^{37–40} Therefore, combining these Bcl-x1 family inhibitors with zotatifin could offer a more effective therapeutic strategy. Our experimental results corroborated this hypothesis. Indeed, while neither zotatifin nor Bcl-x1 inhibitors alone produced significant antitumor effects in iCCAOs, their combination markedly triggered apoptosis. These findings suggest a potent synergistic interaction between zotatifin and Bcl-x1 inhibitors, which could be crucial for overcoming resistance mechanisms and enhancing therapeutic efficacy in iCCA. The observed consistency in response across the two patient-derived organoid models supports the reproducibility of our findings; nonetheless, validation in a larger cohort of patient-derived models is warranted to confirm their reliability and importance for developing personalized approaches against iCCA. Thus, our study highlights the potential of targeting eIF4A1 in iCCA, both as a single agent and in combination with Bcl-x1 inhibitors.

Although these findings open new avenues for developing more effective therapeutic approaches, future studies should focus on *in vivo* validation and clinical trials to confirm the efficacy and safety profiles of these therapies in

patients with iCCA. Nonetheless, in cohorts of patients with heavily pretreated metastatic breast cancer, zotatifin displayed anti-tumor activity in combination with fulvestrant and abemaciclib and had a favorable safety profile (NCT04092673), supporting the data and conclusions of our study. Ongoing clinical trials using zotatifin on estrogen

receptor-positive, HER2-negative breast cancer (NCT05101564), estrogen-receptor positive endometrial cancer, low-grade serous ovarian cancer (NCT03675893), and selected advanced solid tumor malignancies, including iCCA (NCT04092673), will further elucidate the usefulness of targeting eIF4A1 as an anticancer strategy.

Affiliations

¹Department of Surgery, Erasmus MC Transplant Institute, University Medical Center Rotterdam, Rotterdam, the Netherlands; ²Department of Medicine, Surgery, and Pharmacy, University of Sassari, Sassari, Italy; ³Department of Biomedical Sciences, University of Sassari, Sassari, Italy; ⁴National Institute of Gastroenterology, IRCCS Saverio de Bellis, Castellana Grotte, Italy; ⁵Institute of Pathology, University of Regensburg, Regensburg, Germany; ⁶Department of Biomedical Sciences, University of Cagliari, Cagliari, Italy; ⁷Department of Gastroenterology, Hepatology, and Endocrinology, Hannover Medical School, Hannover, Germany

Abbreviations

2-DG, 2-deoxy-D-glucose; 5'-UTR, 5'-untranslated region; BiIIN, biliary epithelial neoplasias; CAF, cancer-associated fibroblast; ECAR, extracellular acidification rate; eIF4A1, eukaryotic initiation factor 4A1; eIF, eukaryotic initiation factor; FCCP, carbonyl cyanide-p-trifluoromethoxyphenylhydrazone; hCAF, human intrahepatic cancer-associated fibroblast; iCCA, intrahepatic cholangiocarcinoma; iCCAO, iCCA organoid; IPBN, intraductal papillary biliary neoplasms; OCR, oxygen consumption rate; PER, total proton efflux rate; PHB1, prohibitin 1; PI, propidium iodide; Rot, rotenone; SEER, Surveillance, Epidemiology, and End Results; ST, surrounding tissue; T, tumorous; TCGA, The Cancer Genome Atlas.

Financial support

This work was supported by grants from the Italian Association Against Cancer (AIRC; grant number IG 27825); Fondazione di Sardegna 2022-2023, Italy; PRIN 2022, Prot. 2022AHM4AA to DFC; Erasmus MC Human Disease Model Award 2018 (HDMA-380801) to MMAV and LJWvdL; ENW-XS (Project OCENW.XS21.2.003) of the Dutch Research Council to MMAV; Dutch Cancer Society KWF 2022-14364 to MMAV; Dutch Society for Gastroenterology project NVGE-2022 to LJWvdL and MMAV; Cost Action Precision-BTC-Network CA22125 to MMAV; China Scholarship Council No. 202107040034 to WM; AIRC IG 24815 to GG; Deutsche Forschungsgemeinschaft (DFG, German Research Foundation), project n. 493345156, and German Cancer Aid 70114101 to AS. The funders had no role in study design, data collection and analysis, publication decisions, or manuscript preparation.

Conflicts of interest

The authors declare that there are no conflicts of interest regarding the publication of this article.

Please refer to the accompanying ICMJE disclosure forms for further details.

Authors' contributions

DFC, MMAV: designed research and supervised the experimental work. WM, AC, GG, IG, SS, MS, EP, HS, DS, CF: performed all experiments. GLG, LJWvdL, AS, ME: collected and provided human samples, cell lines, organoids, and CAFs. WM, AC, GG, IG, SS, MS, GMP, EP, HS, CF, MMAV, DFC: analyzed the data and interpreted the results. WM, GLG, MMAV, DFC: wrote the manuscript. WM, AC, IG, GLG, ME, LJWvdL, MMAV, DFC: revised the manuscript. WM, LJWvdL, MMAV, DFC: secured funding. All authors reviewed and approved the manuscript before submission.

Data availability statement

All data generated or analyzed during this study are included in this published article (and its supplementary information).

Acknowledgements

The authors are grateful to the patients for providing biomaterials and informed consent for research. We thank the Erasmus MC Biopsy Research Facility at the Department of Surgery (Rotterdam, the Netherlands) for sample processing, storage, and distribution.

Supplementary data

Supplementary data to this article can be found online at <https://doi.org/10.1016/j.jhepr.2025.101416>.

References

Author names in bold designate shared co-first authorship

- [1] Moeini A, Sia D, Bardeesy N, et al. Molecular pathogenesis and targeted therapies for intrahepatic cholangiocarcinoma. *Clin Cancer Res* 2016;22:291–300.
- [2] Banales JM, Marin JGG, Lamarca A, et al. Cholangiocarcinoma 2020: the next horizon in mechanisms and management. *Nat Rev Gastroenterol Hepatol* 2020;17:557–588.
- [3] Kim Y, Moris DP, Zhang X, et al. Evaluation of the 8th edition American Joint Commission on Cancer (AJCC) staging system for patients with intrahepatic cholangiocarcinoma: a surveillance, epidemiology, and end results (SEER) analysis. *J Surg Oncol* 2017;116:643–650.
- [4] Bertuccio P, Malvezzi M, Carioli G, et al. Global trends in mortality from intrahepatic and extrahepatic cholangiocarcinoma. *J Hepatol* 2019;71:104–114.
- [5] Abou-Alfa GK, Sahai V, Hollebecque A, et al. Pemigatinib for previously treated, locally advanced or metastatic cholangiocarcinoma: a multicentre, open-label, phase 2 study. *Lancet Oncol* 2020;21:671–684.
- [6] Makawita S, Abou-Alfa GK, Roychowdhury S, et al. Infigratinib in patients with advanced cholangiocarcinoma with FGFR2 gene fusions/translocations: the PROOF 301 trial. *Future Oncol* 2020;16:2375–2384.
- [7] Goyal L, Meric-Bernstam F, Hollebecque A, et al. Futibatinib for FGFR2-rearranged intrahepatic cholangiocarcinoma. *N Engl J Med* 2023;388:228–239.
- [8] Abou-Alfa GK, Macarulla T, Javle MM, et al. Ivosidenib in IDH1-mutant, chemotherapy-refractory cholangiocarcinoma (ClarIDHy): a multicentre, randomised, double-blind, placebo-controlled, phase 3 study. *Lancet Oncol* 2020;21:796–807.
- [9] Braconi C, Roessler S, Kruk B, et al. Molecular perturbations in cholangiocarcinoma: is it time for precision medicine? *Liver Int* 2019;39(Suppl 1):32–42.
- [10] Silvera D, Formenti SC, Schneider RJ. Translational control in cancer. *Nat Rev Cancer* 2010;10:254–266.
- [11] Robichaud N, Sonenberg N, Ruggero D, et al. Translational control in cancer. *Cold Spring Harb Perspect Biol* 2019;11:a032896.
- [12] Jackson RJ, Hellen CU, Pestova TV. The mechanism of eukaryotic translation initiation and principles of its regulation. *Nat Rev Mol Cell Biol* 2010;11:113–127.
- [13] Fabbri L, Chakraborty A, Robert C, et al. The plasticity of mRNA translation during cancer progression and therapy resistance. *Nat Rev Cancer* 2021;21:558–577.
- [14] Rubio CA, Weisburd B, Holderfield M, et al. Transcriptome-wide characterization of the eIF4A signature highlights plasticity in translation regulation. *Genome Biol* 2014;15:476.
- [15] **Chan K, Robert F, Oertlin C**, et al. eIF4A supports an oncogenic translation program in pancreatic ductal adenocarcinoma. *Nat Commun* 2019;10:5151.
- [16] **Lin CJ, Nasr Z**, Prensirut PK, et al. Targeting synthetic lethal interactions between Myc and the eIF4F complex impedes tumorigenesis. *Cell Rep* 2012;1:325–333.
- [17] Nishida Y, Zhao R, Heese LE, et al. Inhibition of translation initiation factor eIF4a inactivates heat shock factor 1 and exerts anti-leukemia activity in AML. *Leukemia* 2021;35:2469–2481.
- [18] Iwasaki S, Iwasaki W, Takahashi M, et al. The translation inhibitor rocaglamide targets a bimolecular cavity between eIF4A and polypurine RNA. *Mol Cell* 2019;73:738–748.
- [19] Iwasaki S, Floor SN, Ingolia NT. Rocaglates convert DEAD-box protein eIF4A into a sequence-selective translational repressor. *Nature* 2016;534:558–561.

- [20] Chu J, Zhang W, Cencic R, et al. Amidino-rocaglates: a potent class of eIF4A inhibitors. *Cell Chem Biol* 2019;26:1586–1593.
- [21] **Wolfe AL, Singh K, Zhong Y, et al.** RNA G-quadruplexes cause eIF4A-dependent oncogene translation in cancer. *Nature* 2014;513:65–70.
- [22] Zhao N, Kabotyanski EB, Saltzman AB, et al. Targeting eIF4A triggers an interferon response to synergize with chemotherapy and suppress triple-negative breast cancer. *J Clin Invest* 2023;133:e172503.
- [23] **Liang S, Zhou Y, Chen Y, et al.** Decreased expression of EIF4A1 after preoperative brachytherapy predicts better tumor-specific survival in cervical cancer. *Int J Gynecol Cancer* 2014;24:908–915.
- [24] Modelska A, Turro E, Russel R, et al. The malignant phenotype in breast cancer is driven by eIF4A1-mediated changes in the translational landscape. *Cell Death Dis* 2015;6:e1603.
- [25] **Steinmann SM, Sánchez-Martín A, Tanzer E, et al.** eIF4A1 is a prognostic marker and actionable target in human hepatocellular carcinoma. *Int J Mol Sci* 2023;24:2055.
- [26] Gao C, Guo X, Xue A, et al. High intratumoral expression of eIF4A1 promotes epithelial-to-mesenchymal transition and predicts unfavorable prognosis in gastric cancer. *Acta Biochim Biophys Sin* 2020;52:310–319.
- [27] Ernst JT, Thompson PA, Nilewski C, et al. Design of development candidate eFT226, a first in class inhibitor of eukaryotic initiation factor 4A RNA helicase. *J Med Chem* 2020;63:5879–5955.
- [28] Broutier L, Mastrogiovanni G, Versteegen MMA, et al. Human primary liver cancer-derived organoid cultures for disease modeling and drug screening. *Nat Med* 2017;23:1424–1435.
- [29] van Tienderen GS, Rosmark O, Lieshout R, et al. Extracellular matrix drives tumor organoids toward desmoplastic matrix deposition and mesenchymal transition. *Acta Biomater* 2023;158:115–131.
- [30] **Lieshout R, Kamp EJCA, Versteegen MMA, et al.** Cholangiocarcinoma cell proliferation is enhanced in primary sclerosing cholangitis: a role for IL-17A. *Int J Cancer* 2023;152:2607–2614.
- [31] Scheiter A, Hierl F, Winkel I, et al. Wnt/ β -catenin-pathway alterations and homologous recombination deficiency in cholangiocarcinoma cell lines and clinical samples: towards specific vulnerabilities. *J Pers Med* 2022;12:1270.
- [32] **Saborowski A, Wolff K, Spielberg S, et al.** Murine liver organoids as a genetically flexible system to study liver cancer in vivo and in vitro. *Hepatol Commun* 2019;3:423–436.
- [33] DeGregori J, Johnson DG. Distinct and overlapping roles for E2F family members in transcription, proliferation and apoptosis. *Curr Mol Med* 2006;6:739–748.
- [34] Lizardo MM, Hughes C, Huang YZ, et al. Pharmacologic inhibition of EIF4A blocks NRF2 synthesis to prevent osteosarcoma metastasis. *Cancer Res* 2024;30:4464–4481.
- [35] **Czabotar PE, Garcia-Saez AJ.** Mechanisms of BCL-2 family proteins in mitochondrial apoptosis. *Nat Rev Mol Cell Biol* 2023;24:732–748.
- [36] Hoffmeister-Wittmann P, Mock A, Nichetti F, et al. Bcl-x(L) as prognostic marker and potential therapeutic target in cholangiocarcinoma. *Liver Int* 2022;42:2855–2870.
- [37] Levenson JD, Phillips DC, Mitten MJ, et al. Exploiting selective BCL-2 family inhibitors to dissect cell survival dependencies and define improved strategies for cancer therapy. *Sci Transl Med* 2015;7:279ra40.
- [38] Sarosiek KA, Chi X, Bachman JA, et al. BID preferentially activates BAK while BIM preferentially activates BAX, affecting chemotherapy response. *Mol Cell* 2013;51:751–765.
- [39] **Thummuri D, Khan S, Underwood PW, et al.** Overcoming gemcitabine resistance in pancreatic cancer using the BCL-X(L)-specific degrader DT2216. *Mol Cancer Ther* 2022;21:184–192.
- [40] **Khan S, Zhang X, Lv D, et al.** A selective BCL-X(L) PROTAC degrader achieves safe and potent antitumor activity. *Nat Med* 2019;25:1938–1947.

Keywords: Biliary tumors; EIF4A1; Zotatifin; Bcl-xl.

Received 26 June 2024; received in revised form 27 March 2025; accepted 27 March 2025; Available online 3 April 2025